

Fully Implicit Multidimensional Hybrid Upwind Scheme for Coupled Flow and Transport with Buoyancy

François Hamon^a and Brad Mallison^b

^a Lawrence Berkeley National Laboratory (now with Total)

^b Chevron ETC

March 13th, 2019

1. Implicit Hybrid Upwinding for Coupled Flow and Transport
2. MultiD-IHU Finite-Volume Scheme
3. Numerical Examples

Coupled Multiphase Flow and Transport at the Darcy Scale

Constitutive equations:

Coupled flow and transport of two immiscible and incompressible phases:

Mass conservation:
$$\phi \frac{\partial S_\ell}{\partial t} + \nabla \cdot \mathbf{u}_\ell(p, S) = q_\ell$$

Darcy's law:
$$\mathbf{u}_\ell(p, S) = -k \lambda_\ell(S) \nabla \Phi_\ell = -k \lambda_\ell(S) (\nabla p - \mathbf{g}_\ell)$$

$$\lambda_\ell(S) = k_{r\ell}(S) / \mu_\ell \quad (\text{mobility})$$

$$\mathbf{g}_\ell = \rho_\ell g \nabla z \quad (\text{gravity weight})$$

Elliptic-hyperbolic system of PDEs:

$$\left\{ \begin{array}{l} \nabla \cdot \mathbf{u}_T(p, S) = q_T \quad \text{with } \mathbf{u}_T = \sum_\ell \mathbf{u}_\ell \\ \phi \frac{\partial S_\ell}{\partial t} + \nabla \cdot \left(\frac{\lambda_\ell}{\lambda_T} \mathbf{u}_T(p, S) + k \sum_m \frac{\lambda_m \lambda_\ell}{\lambda_T} (\mathbf{g}_\ell - \mathbf{g}_m) \right) = q_\ell \end{array} \right.$$

Fully Implicit Finite-Volume Discretization

Backward-Euler FV discretization:

$$\left\{ \begin{array}{l} \sum_{j \in \text{adj}(i)} u_{T,ij} = V_i q_{T,i} \\ V_i \phi_i \frac{S_{\ell,i}^{n+1} - S_{\ell,i}^n}{\Delta t} + \sum_{j \in \text{adj}(i)} F_{\ell,ij}^{n+1} = V_i q_{\ell,i} \end{array} \right.$$

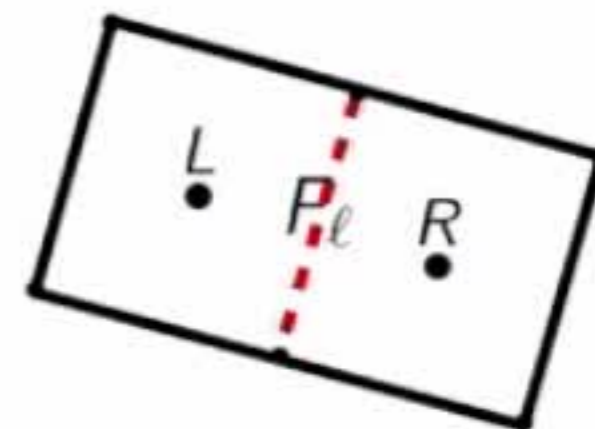
Motivation for implicitness: very large CFL numbers

Numerical flux:

Approximates the phase velocity at interface (LR):

$$F_{\ell,LR}^{n+1} \approx \int_{\Gamma_{LR}} \mathbf{u}_{\ell}^{n+1}(\mathbf{x}, p, S_1, S_2) \cdot \mathbf{n}_{LR} d\Gamma_{LR}$$

- ▷ Elliptic term: TPFA discretization
- ▷ Hyperbolic coefficients: we address two issues
 - Improving nonlinear convergence
 - Achieving sufficient accuracy for practical applications



1D Upwinding Strategies

Hyperbolic coefficients discretized using the two adjacent saturations S_L and S_R

1D Phase-Potential Upwinding:

- ▷ Viscous and buoyancy terms upwinded together using phase potentials
- ▷ Discontinuous flux derivatives cause Newton convergence issues

1D Implicit Hybrid Upwinding:

- ▷ Separate treatment of viscous and buoyancy terms
- ▷ Differentiable numerical flux

$$\begin{aligned}
 F_{\ell,LR}^{n+1} &\approx \int_{\Gamma_{LR}} \frac{\lambda_\ell}{\lambda_T} \mathbf{u}_T(p, S) \cdot \mathbf{n}_{LR} d\Gamma_{LR} \\
 &+ \sum_m \int_{\Gamma_{LR}} k \frac{\lambda_m \lambda_\ell}{\lambda_T} (\mathbf{g}_\ell - \mathbf{g}_m) \cdot \mathbf{n}_{LR} d\Gamma_{LR} \\
 &= \underbrace{V_{\ell,LR}^{n+1}}_{\text{viscous part}} + \underbrace{G_{\ell,LR}^{n+1}}_{\text{buoyancy part}}
 \end{aligned}$$

[Eymard *et al.*, 1989]

[Lee *et al.*, 2015; Lee & Efendiev, 2016, 2018]

[H. & Tchelepi, 2016; H., Mallison, Tchelepi 2016, 2018]

[Moncorgé *et al.*, 2018]

Implicit Hybrid Upwinding (1D-IHU) – Viscous and Buoyancy Parts

Viscous term:

$$V_{\ell,LR}^{n+1} \approx \int_{\Gamma_{LR}} \frac{\lambda_{\ell}}{\sum_m \lambda_m} \mathbf{u}_T(p, S) \cdot \mathbf{n}_{LR} d\Gamma_{LR}$$

$$= \frac{\lambda_{\ell}^V}{\sum_m \lambda_m^V} u_{T,LR}$$

Upwinding based on the sign of $u_{T,LR}$:

$$\lambda_{\ell}^V(S_L, S_R) = \begin{cases} \lambda_{\ell}(S_L) & \text{if } u_{T,LR} > 0 \\ \lambda_{\ell}(S_R) & \text{otherwise} \end{cases}$$

Buoyancy term:

$$G_{\ell,LR}^{n+1} \approx \sum_m \int_{\Gamma_{LR}} k \frac{\lambda_{\ell} \lambda_m}{\lambda_T} (\mathbf{g}_{\ell} - \mathbf{g}_m) \cdot \mathbf{n}_{LR} d\Gamma_{LR}$$

$$= T_{LR} \sum_m \frac{(\lambda_{\ell} \lambda_m)^G}{\lambda_T^G} (g_{\ell,LR} - g_{m,LR})$$

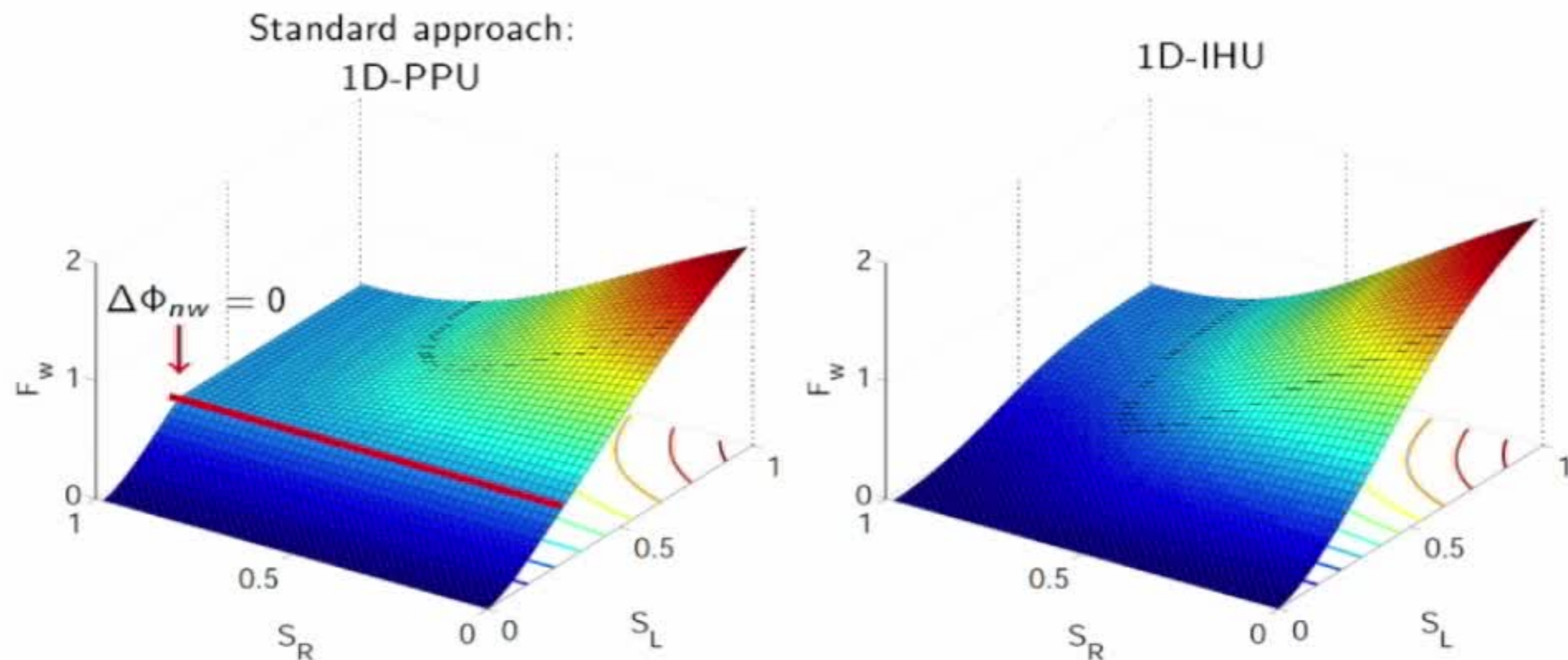
Directionality based on density differences:

$$(\lambda_{\ell} \lambda_m)^G = \begin{cases} \lambda_{\ell}(S_L) \lambda_m(S_R) & \text{if } (\rho_{\ell} - \rho_m)(z_R - z_L) > 0 \\ \lambda_{\ell}(S_R) \lambda_m(S_L) & \text{otherwise} \end{cases}$$

1D-PPU and 1D-IHU Numerical Fluxes

1D-IHU flux properties:

- ▷ Differentiable, monotone, and consistent numerical flux



1D-IHU improves nonlinear convergence:

- ▷ Fully Implicit [Lee *et al.*, 2015; Lee & Efendiev, 2016; H. & Tchelepi, 2016; H., Mallison, Tchelepi 2016, 2018]
- ▷ Sequential Fully Implicit [Moncorgé *et al.*, 2018; Lee & Efendiev, 2018]

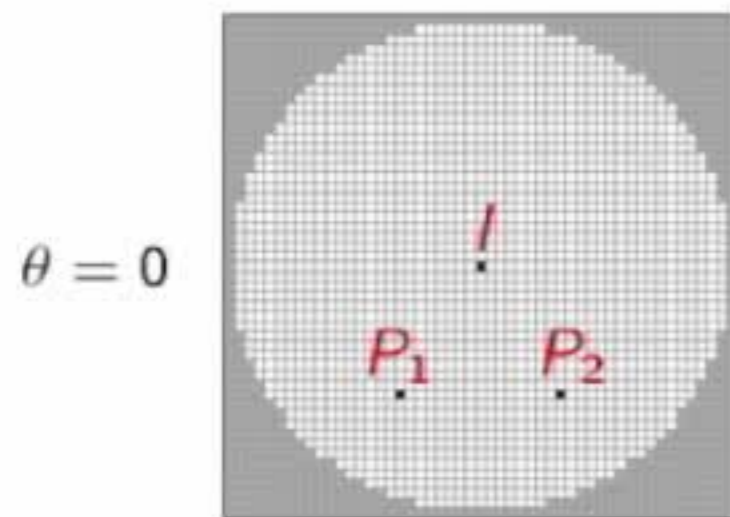
Grid Orientation Effect (GOE) in Reservoir Simulation

Limited accuracy of 1D-PPU and 1D-IHU:

- ▷ High sensitivity of the flow pattern to grid orientation
- ▷ Severe GOE for adverse mobility ratios

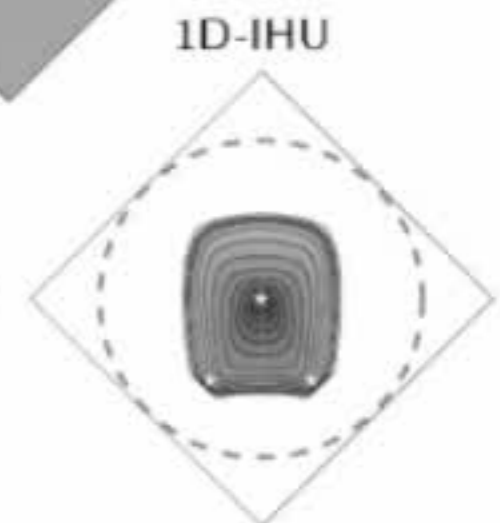
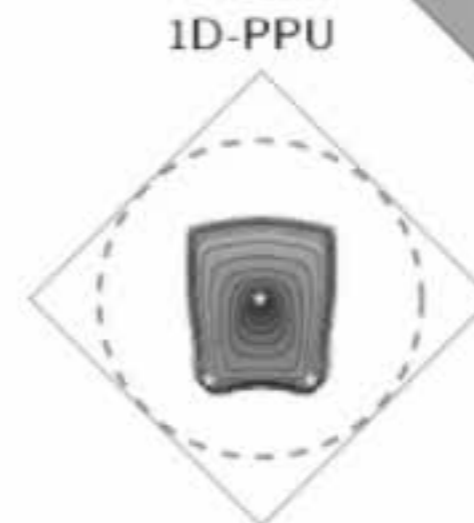
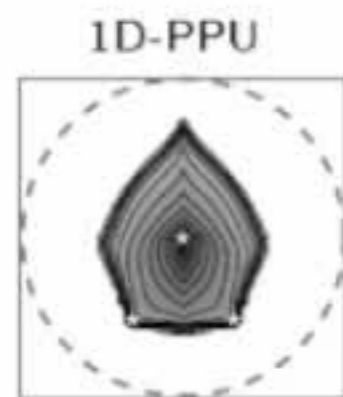
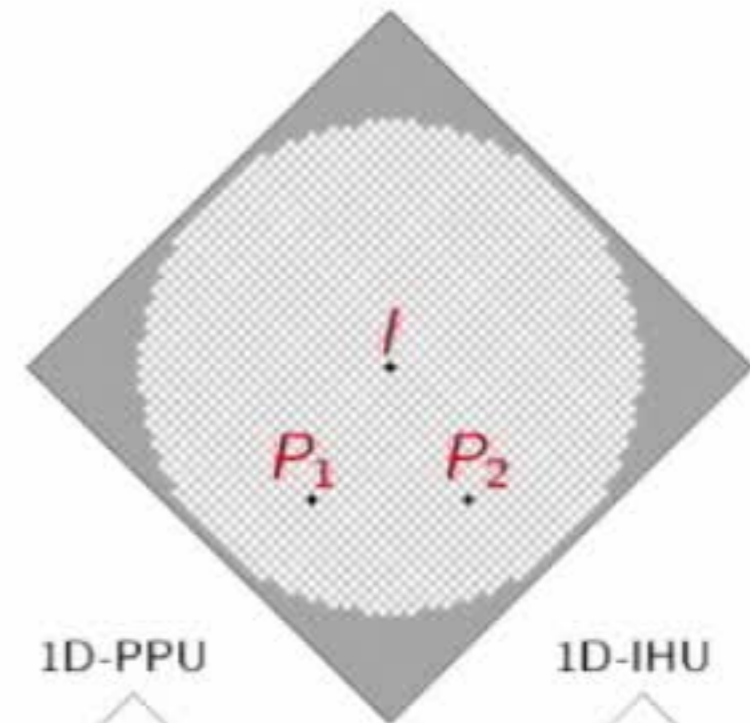
[Bell & Shubin, 1984; Brand *et al.*, 1991; Eymard, Guichard, Masson, 2012; etc]

Three-well problem with buoyancy:



$$\frac{\mu_{nw}}{\mu_w} = 100$$

$\theta = \frac{\pi}{4}$



[Kozdon *et al.*, 2011(a,b)]

MultiD-IHU Finite-Volume Scheme

Goal: Reducing GOE while preserving robust nonlinear convergence

Methodology:

- ▷ Split viscous and buoyancy upwinding
- ▷ Larger adaptive stencil for mobility evaluation

Interaction regions:

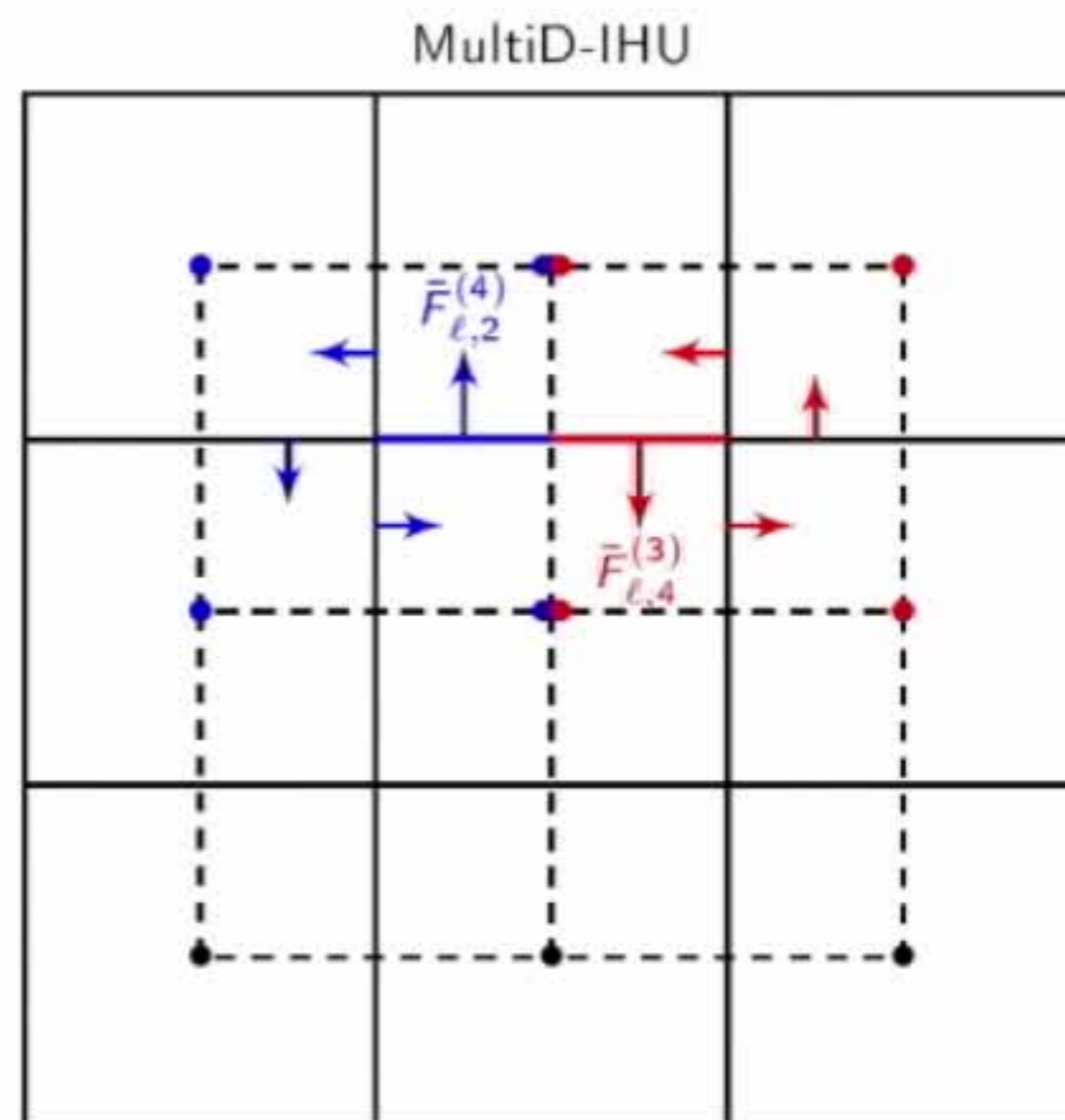
- ▷ Flux decomposition into half fluxes

$$F_{\ell,ij} = \bar{F}_{\ell,k}^{(k+2)} - \bar{F}_{\ell,k-2}^{(k+1)}$$

- ▷ In each interaction region:
 - Half fluxes depend on up to four saturations
 - Coupling of the half fluxes based on flow direction

MultiD-PPU: [Kozdon *et al.*, 2011; Keilegavlen *et al.*, 2012]

Related approaches: [Arbogast & Huang, 2006; Hurtado, 2007; Lamine & Edwards, 2010, 2013, 2015]



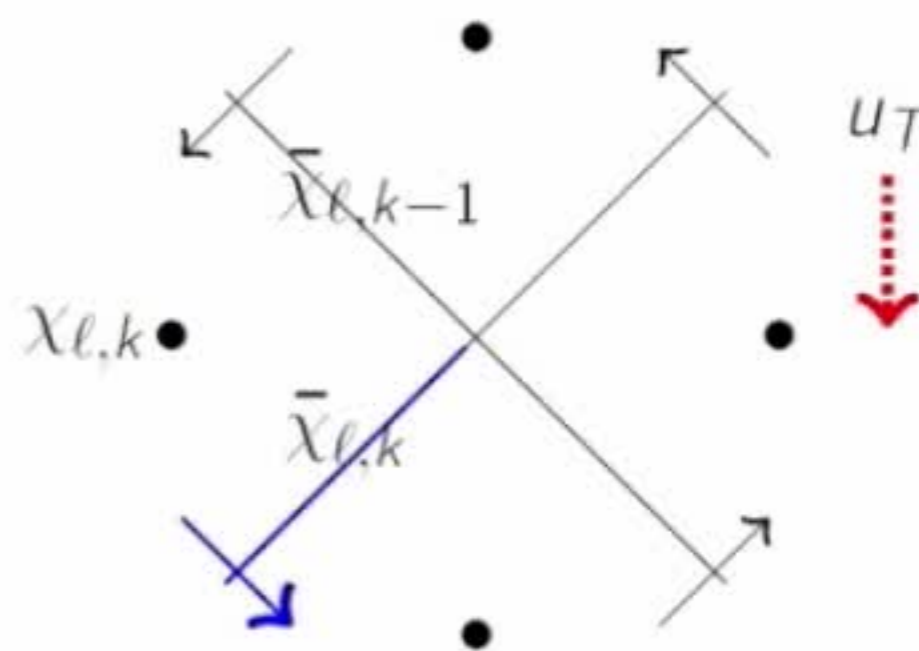
MultiD-IHU Viscous Half Flux (1)

Approximation at half interface k :

$$\begin{aligned}\bar{V}_{\ell,k} &\approx \int_{\Gamma_k} \frac{\lambda_{\ell}}{\lambda_T} \mathbf{u}_T \cdot \mathbf{n}_k d\Gamma_k \\ &= \bar{\chi}_{\ell,k} \bar{u}_{T,k}\end{aligned}$$

where

- ▷ Interfacial mobility ratio: $\bar{\chi}_{\ell,k}$
- ▷ Cell mobility ratio: $\chi_{\ell,k} = \frac{\lambda_{\ell}(S_{\ell,k})}{\lambda_T(S_{\ell,k})}$



Solid arrows show normal directionality at the interface

Adaptive multipoint upwinding:

- ▷ Weighted averaging of mobility ratios
- ▷ Based on upstream cell and interfacial mobility ratios w.r.t $\bar{u}_{T,k}$

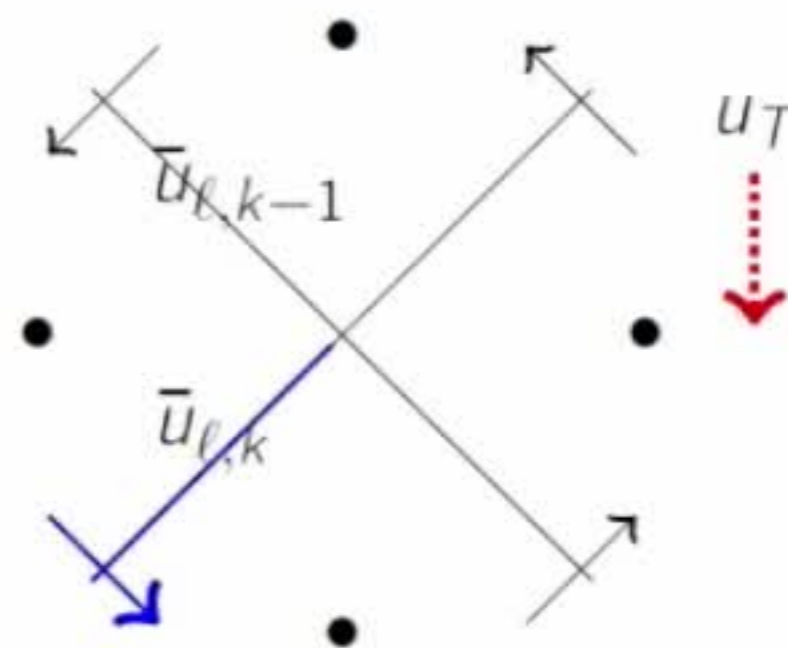
$$\bar{\chi}_{\ell,k} = \begin{cases} (1 - \omega_k^V) \chi_{\ell,k} + \omega_k^V \bar{\chi}_{\ell,k-1} & \text{if } \bar{u}_{T,k} > 0 \\ (1 - \omega_k^V) \chi_{\ell,k+1} + \omega_k^V \bar{\chi}_{\ell,k+1} & \text{otherwise} \end{cases}$$

MultiD-IHU Viscous Half Flux (2)

Weighting coefficient at half interface k :

- ▷ Accounts for local flow orientation
- ▷ Enforces monotonicity

$$\omega_k^v = \begin{cases} \varphi\left(\max\left(0, \frac{\bar{u}_{T,k-1}}{\bar{u}_{T,k}}\right)\right) & \text{if } \bar{u}_{T,k} > 0 \\ \varphi\left(\max\left(0, \frac{\bar{u}_{T,k+1}}{\bar{u}_{T,k}}\right)\right) & \text{if } \bar{u}_{T,k} < 0 \\ 0 & \text{otherwise} \end{cases}$$



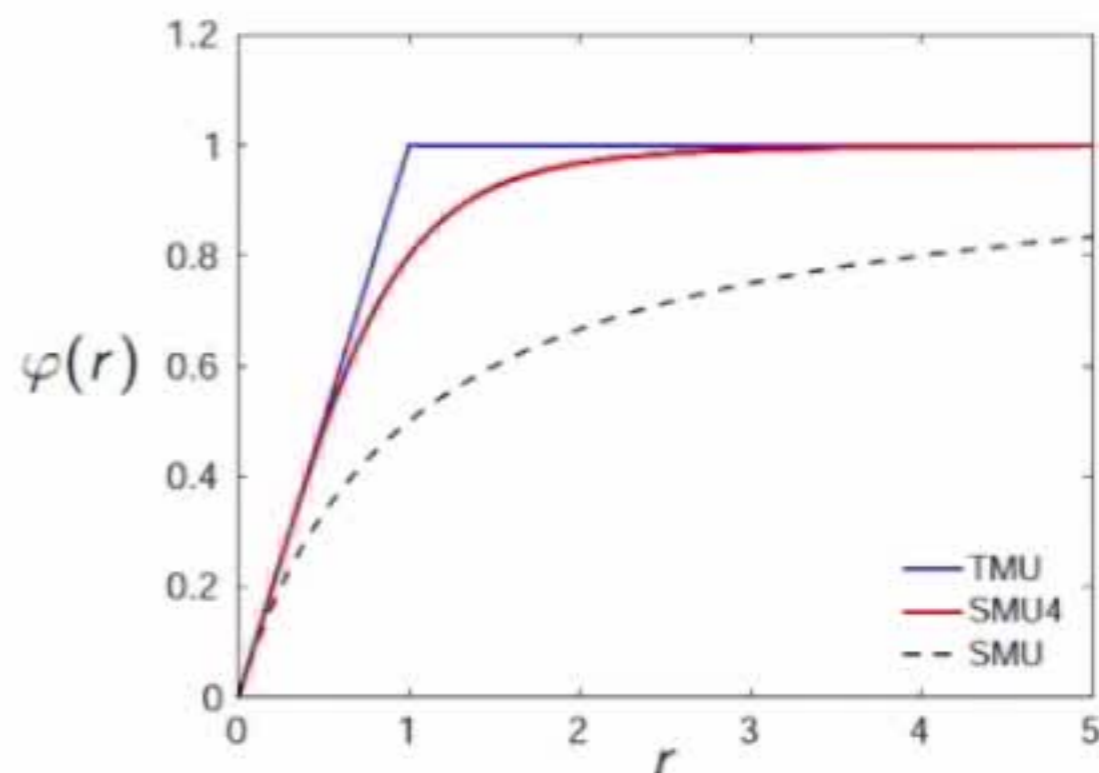
MultiD-IHU limiter:

We consider a new limiter:

- ▷ Reducing transverse diffusion
- ▷ Ensuring differentiability and symmetry

$$\varphi^{SMU4}(r) = \frac{r^4 + r^3 + r^2 + r}{r^4 + r^3 + r^2 + r + 1}$$

Previous work on SMU and TMU limiters: [Koren, 1991; Roe & Sidilkover, 1992; Hurtado *et al.*, 2007; Kozdon *et al.*, 2009]



MultiD-IHU Viscous Half Flux (3)

Mobility ratio coupling:

- ▷ 4×4 linear system in each interaction region

$$\mathbf{A}\bar{\chi}_\ell = \mathbf{B}\chi_\ell$$

- ▷ \mathbf{A} and \mathbf{B} depend on the coefficients ω_k^V

Algorithm:

In each interaction region:

1. Evaluate the four total velocities $\bar{u}_{T,k}$ fully implicitly
2. Evaluate the four cell mobility ratios $\chi_{\ell,k}$
3. Compute interfacial mobility ratios and their derivatives by solving

$$\begin{aligned}\bar{\chi}_\ell &= \mathbf{A}^{-1}\mathbf{B}\chi_\ell \\ \frac{\partial \bar{\chi}_\ell}{\partial \tau_j} &= \mathbf{A}^{-1} \left(-\frac{\partial \mathbf{A}}{\partial \tau_j} \bar{\chi}_\ell + \frac{\partial \mathbf{B}}{\partial \tau_j} \chi_\ell + \mathbf{B} \frac{\partial \chi_\ell}{\partial \tau_j} \right)\end{aligned}$$

4. Evaluate local viscous fluxes and their derivatives

MultiD-IHU Properties

Monotonicity:

For a fixed total velocity field, the numerical flux is monotone

$$\frac{\partial(\bar{F}_{\ell,k} - \bar{F}_{\ell,k-1})}{\partial S_{\ell,j \neq k}} \leq 0 \quad \text{in each interaction region}$$

The proof exploits the limiter properties:

▷ Bounds: $0 \leq \varphi^{SMU4}(r) \leq \min(1, r)$

▷ Symmetry: $\varphi^{SMU4}\left(\frac{1}{r}\right) = \frac{\varphi^{SMU4}(r)}{r}$

Saturation bounds:

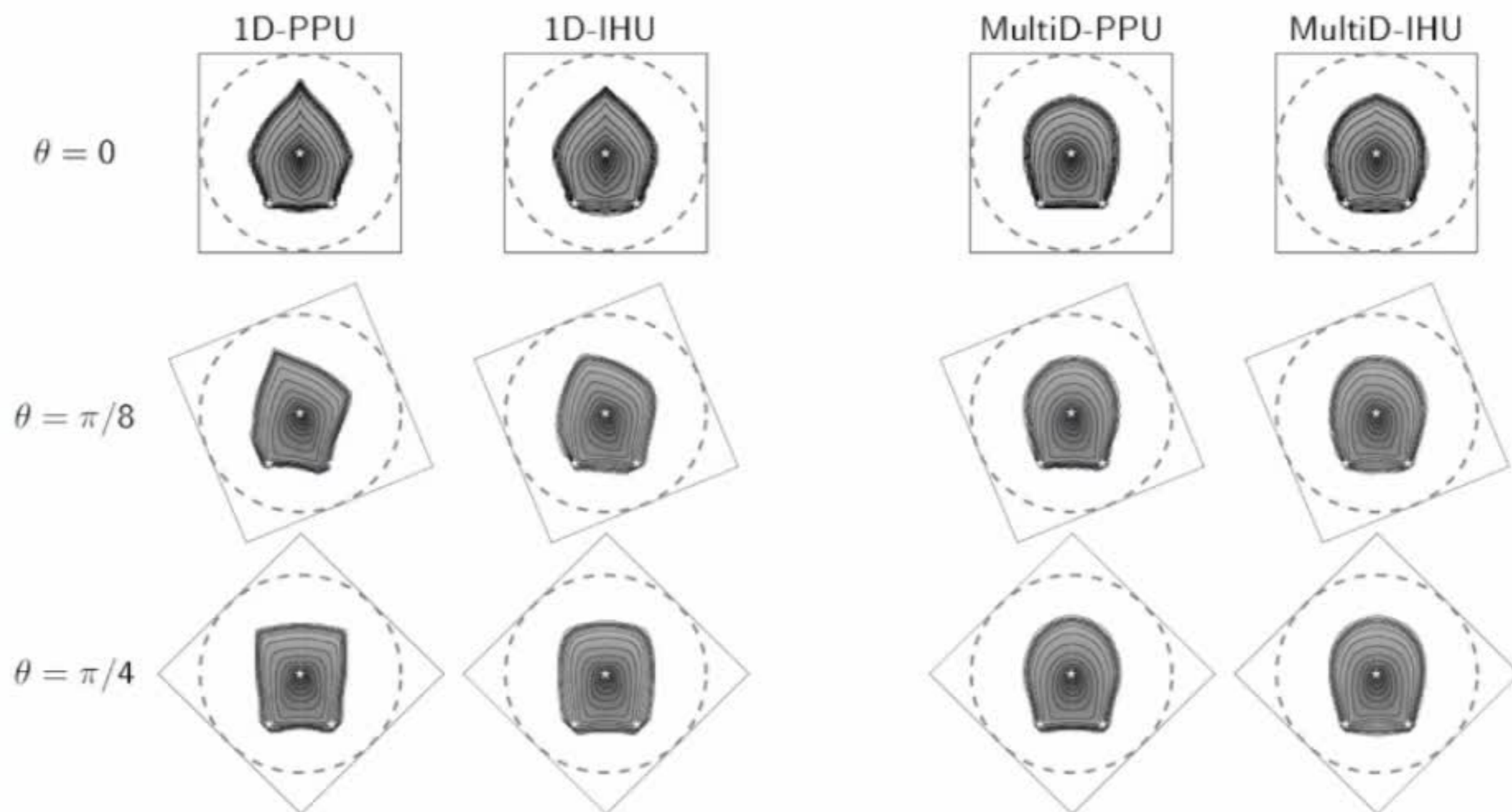
The saturations remain between physical bounds for $n \in \mathbb{N}^+$:

$$0 \leq S_{\ell,i}^n \leq 1$$

Details in [H. & Mallison, 2018, submitted]

Three-Well Problem with Buoyancy – Saturation Maps

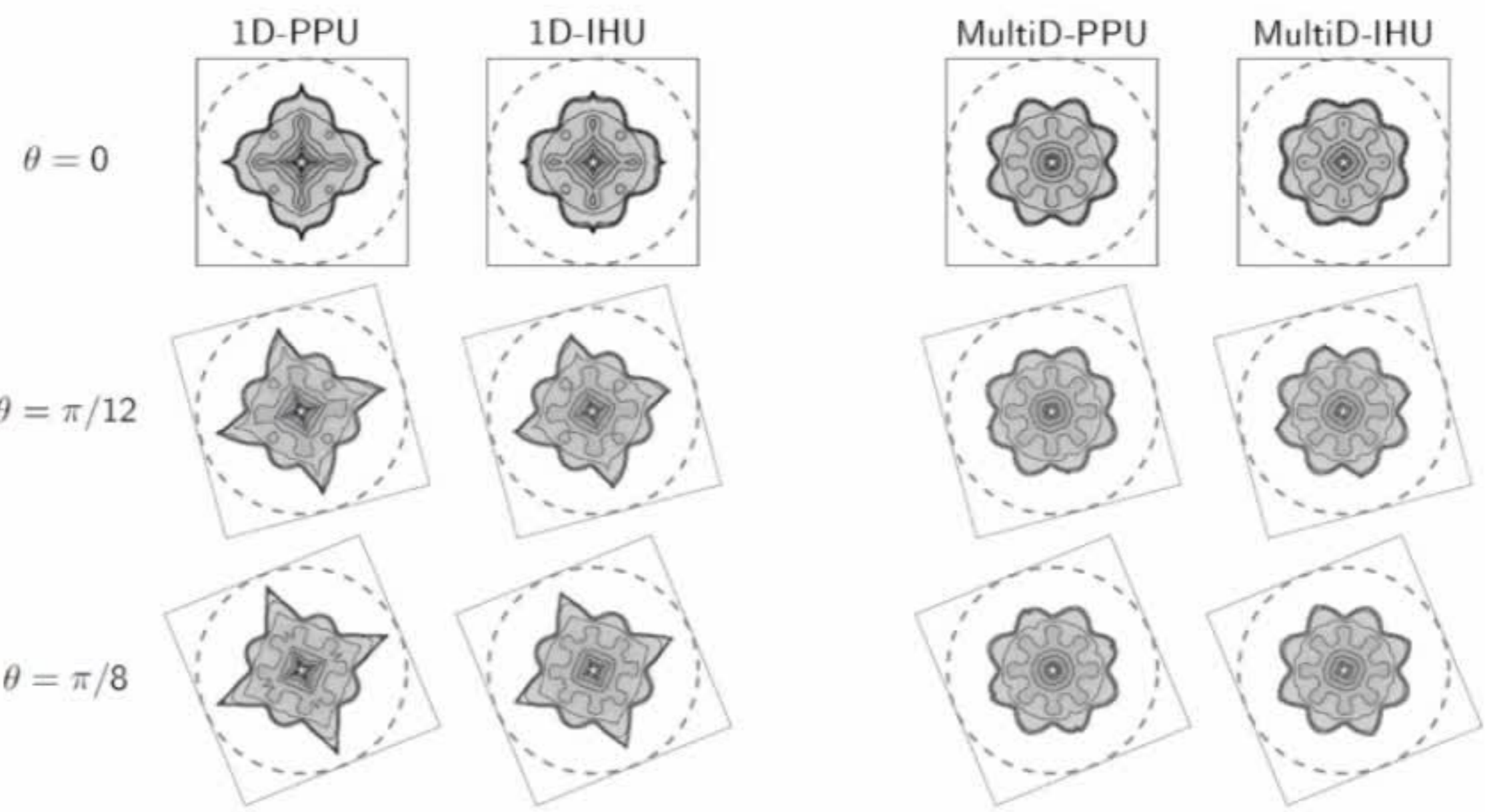
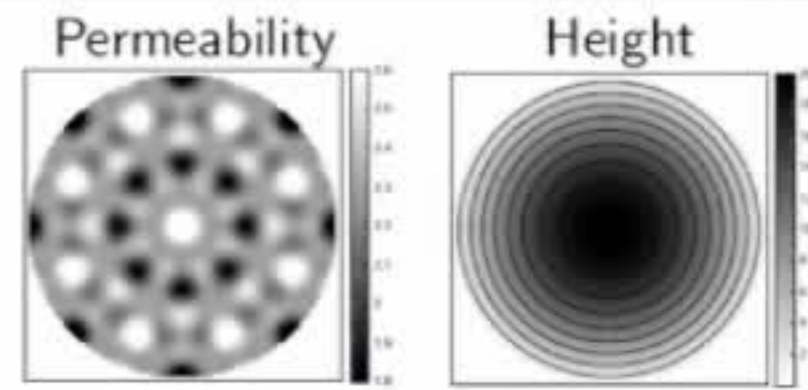
- ▷ MultiD-PPU and MultiD-IHU significantly reduce GOE



$$T = 0.092 \text{ PVI}, \quad \Delta t = 0.0013 \text{ PVI}, \quad \text{CFL} \approx 3.4$$

Heterogeneous Injection with Buoyancy – Saturation Maps

- ▷ Heterogeneous permeability field with eight preferential paths
- ▷ MultiD-PPU and MultiD-IHU are less sensitive to grid orientation



$T = 0.06$ PVI, $\Delta t = 0.0021$ PVI, CFL ≈ 21.1

Heterogeneous Injection with Buoyancy – Nonlinear Behavior

- ▷ MultiD-IHU is the most efficient scheme in terms of nonlinear iterations
- ▷ This is valid for small and for large time steps

θ	1D-PPU	1D-IHU	MultiD-PPU	MultiD-IHU
0	167	161	153	146
$\pi/12$	166	161	154	151
$\pi/8$	167	161	154	153
$\pi/6$	167	161	156	151
$\pi/4$	166	161	154	145

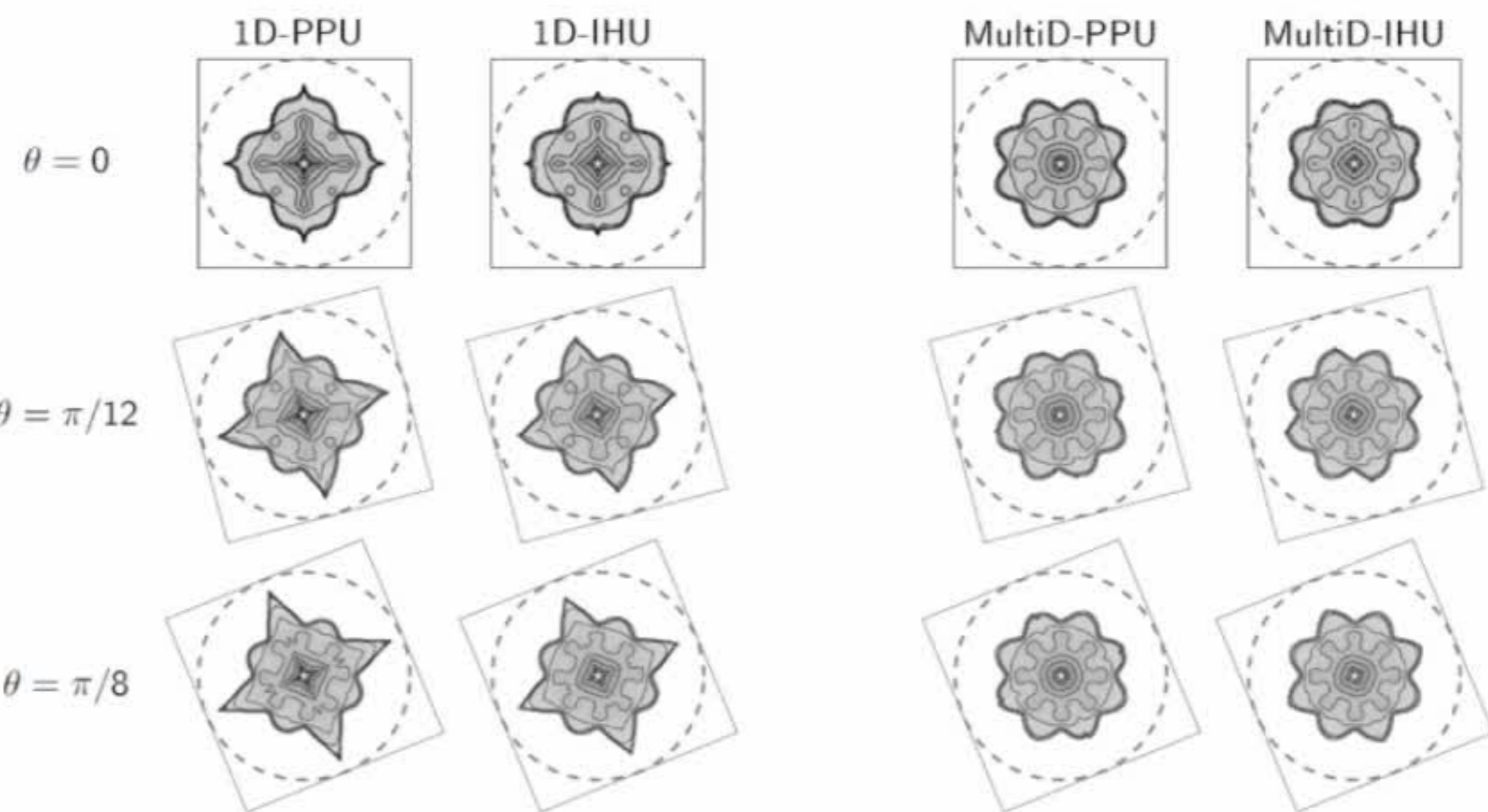
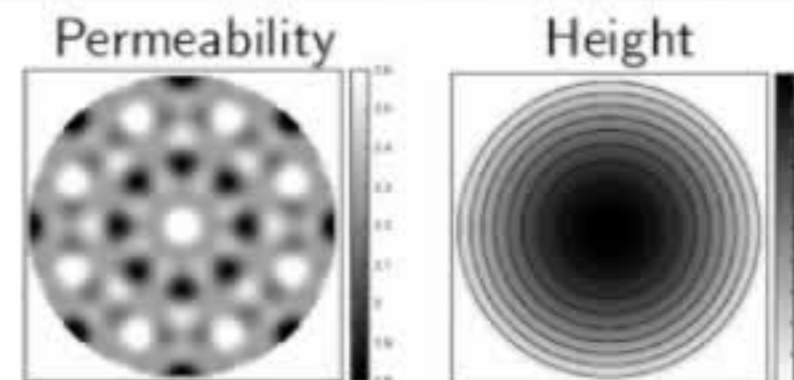
Small time steps: CFL \approx 21.1

θ	1D-PPU	1D-IHU	MultiD-PPU	MultiD-IHU
0	69	72	62	58
$\pi/12$	69	70	61	59
$\pi/8$	72	71	63	62
$\pi/6$	73	71	62	62
$\pi/4$	68	71	61	62

Large time steps: CFL \approx 106.1

Heterogeneous Injection with Buoyancy – Saturation Maps

- ▷ Heterogeneous permeability field with eight preferential paths
- ▷ MultiD-PPU and MultiD-IHU are less sensitive to grid orientation



$T = 0.06$ PVI, $\Delta t = 0.0021$ PVI, CFL ≈ 21.1

Heterogeneous Injection with Buoyancy – Nonlinear Behavior

- ▷ MultiD-IHU is the most efficient scheme in terms of nonlinear iterations
- ▷ This is valid for small and for large time steps

θ	1D-PPU	1D-IHU	MultiD-PPU	MultiD-IHU
0	167	161	153	146
$\pi/12$	166	161	154	151
$\pi/8$	167	161	154	153
$\pi/6$	167	161	156	151
$\pi/4$	166	161	154	145

Small time steps: CFL \approx 21.1

θ	1D-PPU	1D-IHU	MultiD-PPU	MultiD-IHU
0	69	72	62	58
$\pi/12$	69	70	61	59
$\pi/8$	72	71	63	62
$\pi/6$	73	71	62	62
$\pi/4$	68	71	61	62

Large time steps: CFL \approx 106.1

Gravity Segregation with Low-Perm Barriers – Saturation Maps

- ▷ Homogeneous permeability field with horizontal low-perm barriers
- ▷ MultiD-IHU is the least sensitive scheme to GOE

Permeability



CFL ≈ 8.9

$\theta = 0$

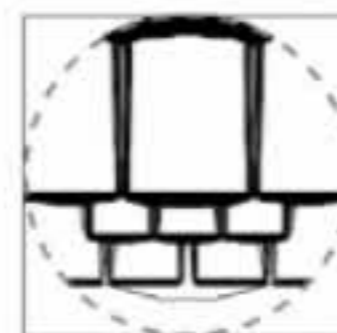
1D-PPU



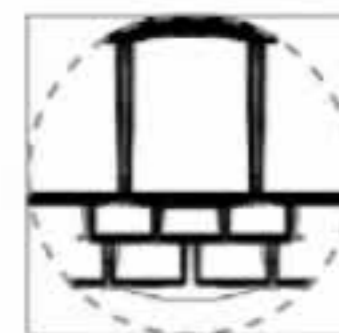
1D-IHU



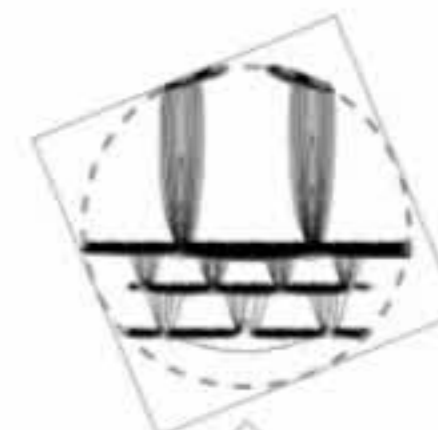
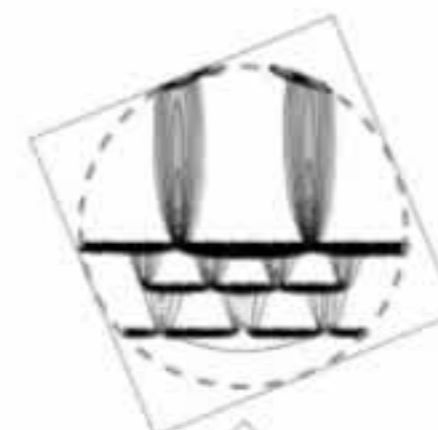
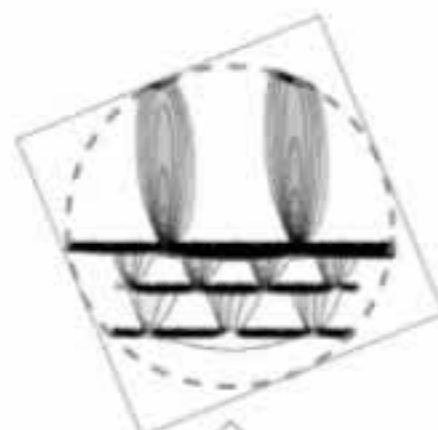
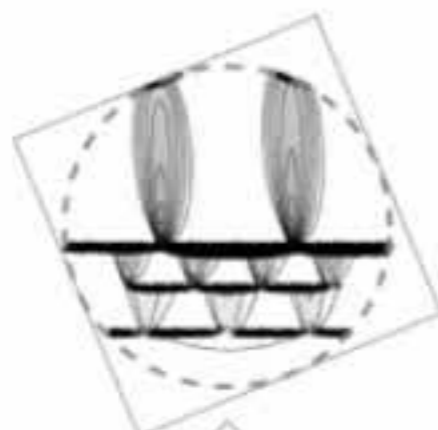
MultiD-PPU



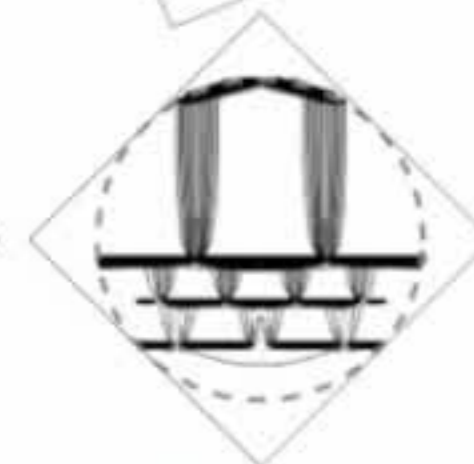
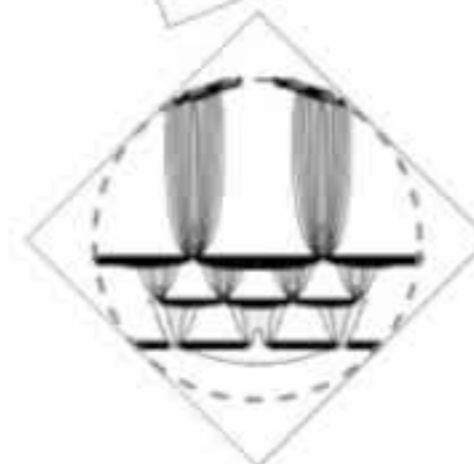
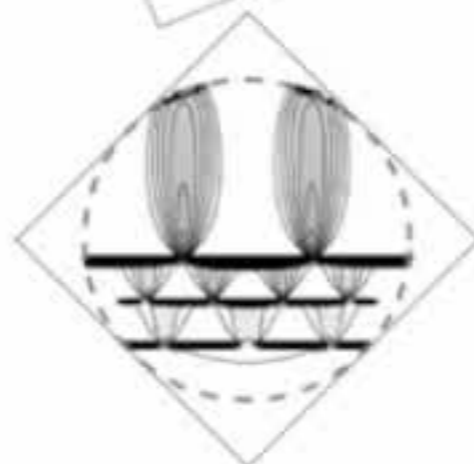
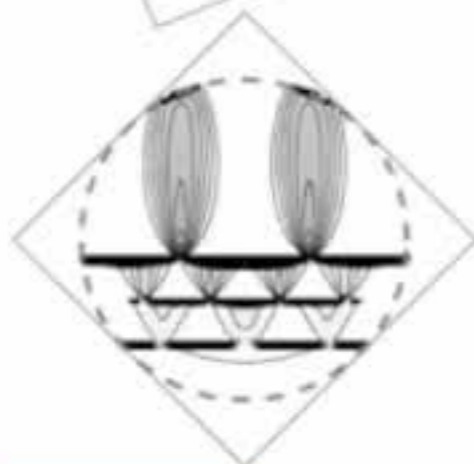
MultiD-IHU



$\theta = \pi/8$



$\theta = \pi/4$



Gravity Segregation with Low-Perm Barriers – Nonlinear Behavior

- ▷ MultiD-IHU is more efficient than both 1D-PPU and MultiD-PPU
- ▷ MultiD-IHU reduces the number of iterations by up to 26 % compared to 1D-PPU

θ	1D-PPU	1D-IHU	MultiD-PPU	MultiD-IHU
0	253	238	257	241
$\pi/12$	307	239	292	235
$\pi/8$	290	234	285	231
$\pi/6$	300	236	290	233
$\pi/4$	281	229	277	229

Small time steps: CFL \approx 8.9

θ	1D-PPU	1D-IHU	MultiD-PPU	MultiD-IHU
0	199	187	202	182
$\pi/12$	244	171	231	167
$\pi/8$	225	174	222	163
$\pi/6$	226	171	228	158
$\pi/4$	212	167	214	151

Large time steps: CFL \approx 17.8